INSTITUT DE FRANCE
Académie des sciences

Comptes Rendus
Physique

Nicolas Noé and François Gaudaire

Numerical modeling of downlink electromagnetic wave exposure generated by 5G beamforming antennas

Volume 22, Special Issue S1 (2021), p. 15-24

Published online: 6 May 2021
Issue date: 30 June 2021

https://doi.org/10.5802/crphys.61

Part of Special Issue: URSI-France 2020 Workshop
Guest editor: Joe Wiart (LTCI, Télécom Paris, Institut Polytechnique de Paris, Institut Mines-Télécom, France)

Les Comptes Rendus. Physique *sont membres du*
Centre Mersenne pour l'édition scientifique ouverte
www.centre-mersenne.org
e-ISSN : 1878-1535

Comptes Rendus
Physique
2021, 22, nº S1, p. 15-24
https://doi.org/10.5802/crphys.61

URSI-France 2020 Workshop / *Journées URSI-France 2020*

Numerical modeling of downlink electromagnetic wave exposure generated by 5G beamforming antennas

Nicolas Noé[*, a] **and François Gaudaire**[b]

[a] CSTB, Division Acoustique Vibration Éclairage et Électromagnétisme, Nantes, France

[b] CSTB, Division Acoustique Vibration Éclairage et Électromagnétisme, Saint-Martin-d'Hères, France

E-mails: nicolas.noe@cstb.fr (N. Noé), francois.gaudaire@cstb.fr (F. Gaudaire)

Abstract. In this paper different scenarios were compared for the numerical modeling of electromagnetic wave exposure to beamforming antennas. These scenarios range from the simplest (using an average radiation pattern) to an almost realistic one (MU-MIMO beamforming taking into account user locations) with intermediate. The results underline the influence of the environment around the antennas on the distribution of the electric field.

Keywords. 5G, Antenna, Beamforming, Exposure, Ray-tracing.

Available online 6th May 2021

1. Introduction

The issue of EMF exposure to smart antennas used for 5G networks was approached as a first step from the point of view of dimensioning security perimeters around antennas. Indeed, to respect the health standards of workers exposure, a security perimeter has to be established around the antenna, inside of which it is prohibited to intervene when the antenna is in operation. Usually this perimeter is determined by calculating the minimum distance around the antenna beyond which the electric field level is always less than the mandatory threshold. This distance is evaluated in free space conditions and hence only depends on the Equivalent Isotropic Radiated Power (EIRP) of emitters.

For beamforming antennas, the antenna gain can vary dynamically up to a maximum gain when a beam is formed in a given direction. Hence using EIRP to compute security perimeters would lead to very long distance. Furthermore in this article we focus on the exposure of the general public in urban environments, beyond the security perimeter.

* Corresponding author.

2. Previous work

While there are several techniques to forecast EMF exposure in urban environments, they mainly rely on measurements [1–3] to feed numerical or statistical models. Therefore, they are not suitable for not-yet existing networks.

In this article we will focus on downlink exposure, leaving aside uplink exposure due to the mobile phone itself. Some metrics [4] exist to handle both simultaneously.

In [5–7] a statistical approach was used to obtain adapted values for security perimeter size for beamforming antennas. In [8] the method consisted in defining different exposure scenarios, depending on a very limited number of parameters: cell type (macro or micro), number of users served simultaneously K and duration of service D. Users were randomly distributed in the environment (80% indoor, 20% outdoor) and the antenna behavior was simulated (at full load) for a set duration of time (6 min) in order to obtain the probability distribution function (pdf) and cumulative distribution function (cdf) of the effective maximum gain of the antenna. The cumulative distribution function of the maximum gain therefore only depended on the chosen parameters. As a consequence this allowed the safety distance to be estimated with a given probability for a maximum level of exposure.

3. A new approach

The previous approach was perfectly suited for security perimeters dimensionning, but it seems insufficient for quantifying public exposure in real urban environments. The question of exposure is not limited to concerns of safety limits. One might indeed try to know precise local exposure (for the search for atypical points in France for example, or for compliance with much more restrictive local laws on the level of exposure such as in the Brussels-Capital region of Belgium). The local exposure may vary greatly depending on the actual configuration of the environment (layout of buildings, construction materials, ...), even for the same type of cell (macro or micro).

With the previous approach, an average diagram could be determined (as a complement to the maximum gain alone). This diagram can be used as an input to a detailed exposure simulation in a given environment, but it is likely that the simulation with the averaged diagram will give results different from the one that could be obtained by averaging the exposure over time.

We therefore propose a new approach to model exposure levels to beamforming antennas, by studying several antenna description scenarios, from the simplest one based on an average antenna diagram to the most complex one by taking into account beamforming operation. The beamforming scenario, being the most realistic, will be used as a the reference scenario.

The main objective of this study is to compare the influence of these different scenarios on electric field exposure level in representative urban environnements.

4. Antenna, environments and simulation method

4.1. *Antenna*

The input antennas can either be a single point with a far field radiation pattern or a set of radiating sub-elements with to model a Uniform Planar Array (UPA) antenna with its beamforming capability. The characteristics of the theoretical UPA antenna used in this study are:

- a 3GPP base element [9] with a 12.6 dBi gain, with a 65° horizontal aperture and a 20° vertical aperture,
- an 8×8 array of base elements with 0.5λ horizontal spacing and 0.6λ vertical spacing,

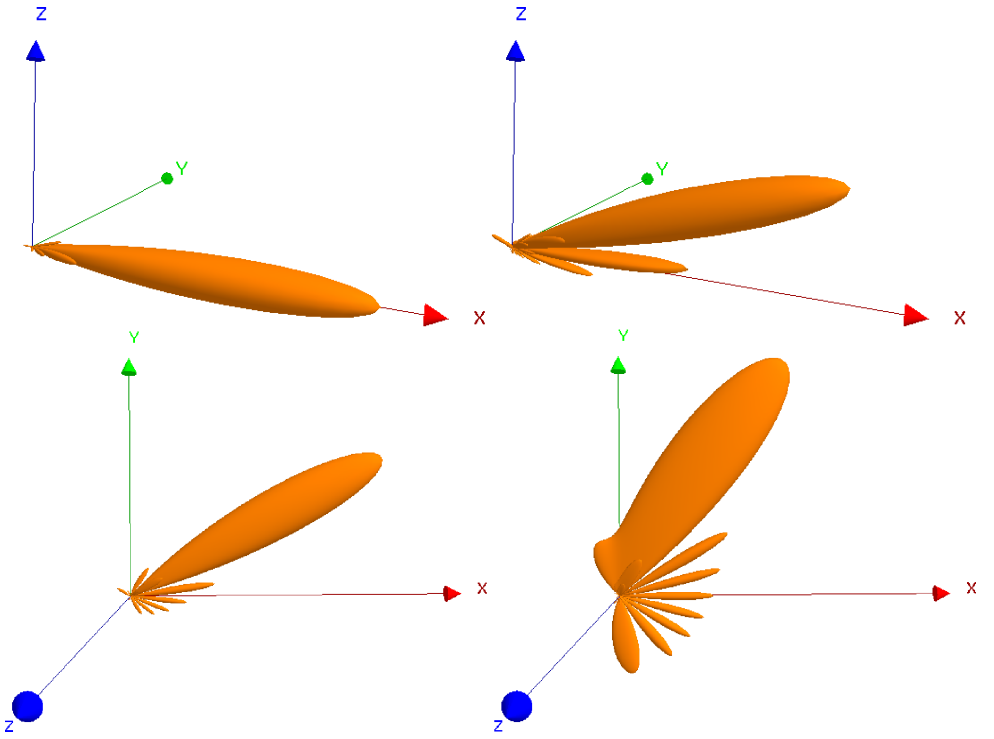

Figure 1. Beamforming to azimuth & tilt: 0° & 0° (top left), 0° & 20° (top right), 30° & 0° (bottom left), 60° & 0° (bottom right), linear scale.

- beams that can be steered from −60° to +60° horizontally and from −20° to +20° vertically,
- a 24.8 dBi gain for a single beam and an input power of 52.04 dBm (160 W).

Beamforming with this antenna is illustrated on Figure 1. It should be noted that the antenna diagram has strong sides lobes for extreme azimuths (close to 60°) since it is a purely analytical model and no side lobes suppression technique was applied.

5. Urban environments

Three different urban environments have been studied (see Figure 2). They were extracted from an exposure simulation study in the city of Paris and represent different configurations: one with mainly line-of-sight (LOS) exposure, one with other building reflections and a canyon street with indirect exposure. Only the buildings in the vicinity of the antenna have been kept (since only one antenna is used). The antenna is mechanically tilted 3° downward.

6. Simulation method

All simulations are performed using a 3D beam-tracing method [10]. This method computes paths between emitters and receivers, taking into account reflection, diffraction and transmission by obstacles, in order to get a complex electric field level (amplitude and phase).

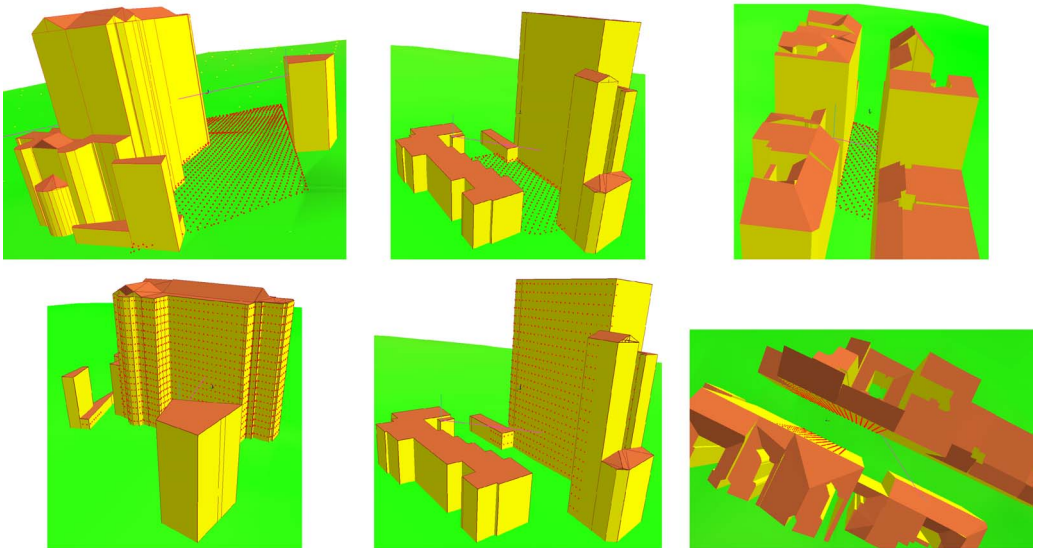

Figure 2. First (left), second (middle) and third (right) environments: antenna with default main lobe direction, ground (top) and facade (bottom) maps of receivers.

7. Scenarios for antenna modeling

7.1. *Scenario 0*

For this scenario a single simulation is performed with an averaged (over all beam directions) far field antenna diagram. This diagram has a 13.17 dBi gain and is illustrated on Figure 3. The averaging is done linearly on the emitted power by sampling the beams every 1° in both directions, hence from $121 \times 41 = 4961$ diagrams ($-60°$ to $60°$ horizontally and $-20°$ to $20°$ vertically).

7.2. *Scenario* $0'$

This slightly more complex scenario is related to the next ANFR guidelines for 5G networks exposure simulation. It is a kind of envelop of all beams, made from the 3GPP base element with a 120° horizontal aperture and a 40° vertical aperture and an (artificial) gain of 24.3 dBi. Once again a single simulation is performed with this diagram and then a 13.5 dB loss factor (defined in the ANFR guidelines [11]) is applied to the final result. This 13.5 dB loss factor fits in with a 1 GB download with a 500 Mbps during a 6 min measurement (hence a 4.4% antenna load).

This diagram is illustrated on Figure 3.

While the shape of the radiation pattern is slightly different from the averaged far field diagram (scenario 0), both scenarios are very similar. Another choice could have been to apply this reduction factor to a maximum envelop of all beams, but this would not significatively change the results.

7.3. *Scenario 1*

In this scenario, beams are formed in every possible direction (whatever the environment). One simulation is performed with a radiation pattern for each beam direction, with a 1° sampling

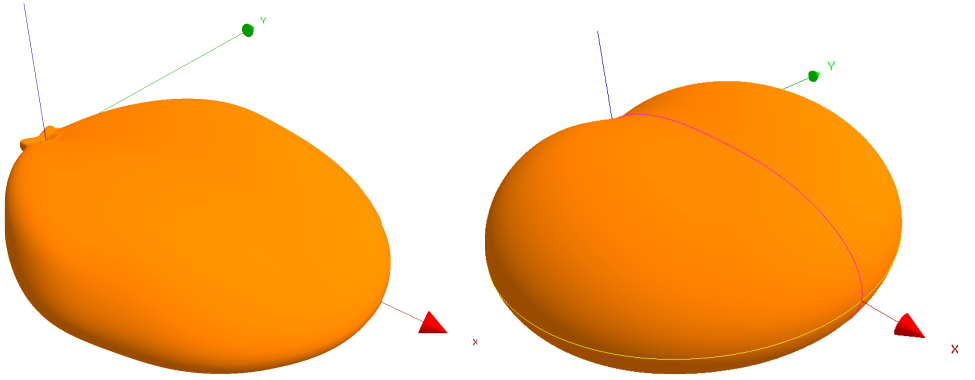

Figure 3. Far field diagrams (linear) used for scenarios 0 (left) and 0′ (right), linear scale.

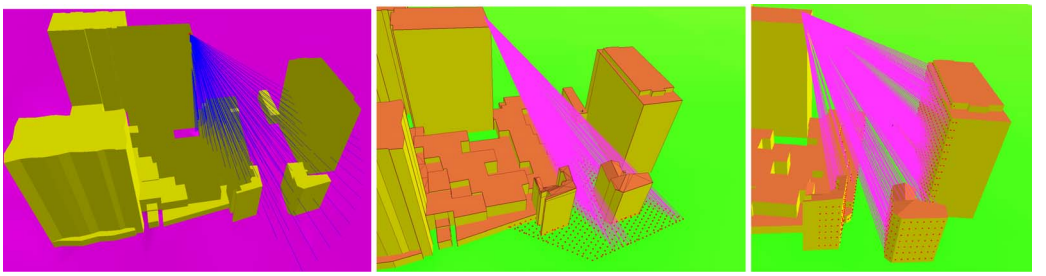

Figure 4. Scenario 1 (left, beams in all possible directions), scenario 1′ (middle and right, beams towards LOS exposure points on the ground and on the facades.

(hence 4961 simulations and exposure maps) as illustrated on Figure 4. In this scenario each beam has the same probability, not taking into account user location. That is to say that beams can be formed in directions where no user stands (toward the sky for instance).

Then an average exposure map is computed to compare with other scenarios. The averaged electric field is one again computed with a linear averaging on the power density.

7.4. *Scenario* 1′

A smart antenna is assumed to form beams in the direction of standing users. A rough approximation is to consider only beams pointing to exposure points (either on the ground or on the building frontages) that are in line-of-sight of the antenna. As a matter of fact users are either in the streets or in the building, and not floating in air yet.[1] The main point of this scenario is that it is easy to set up without any change in simulation tools, as it is only a sub-case of scenario 1. For the studied environments, LOS exposure points represent 10% of the ground surface and 20% of the facades (mainly the building in front of the antenna) as illustrated on Figure 4.

This scenario likely overestimates exposure, as the full power of the antenna is concentrated toward the exposure areas in LOS.

[1] That might change in the future with drones using mobile telephony network.

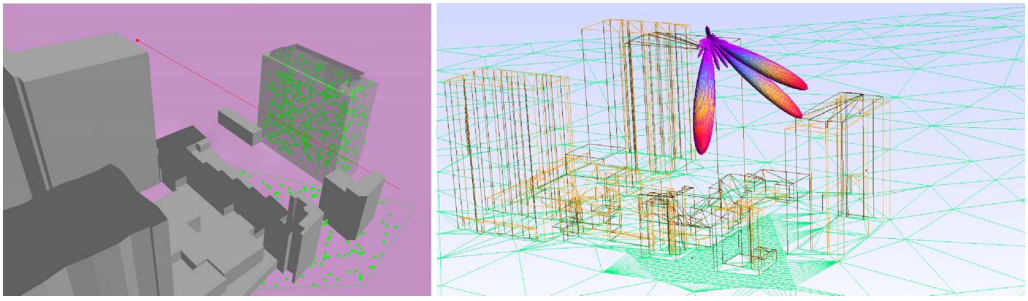

Figure 5. Scenario 2′: randomly generated UEs (left) and MU-MIMO beamforming for $K = 3$ served UEs (right).

7.5. *Scenario 2*

In this scenario, users are taken into account and beamforming is dynamically computed depending on the channel between the antennas sub-elements and the users. It aims to reproduce the real behaviour of a MU-MIMO beamforming antenna. The methods used to simulate such a behaviour are detailed in the following sections. In this scenario exposure points and user locations are independant.

The time dimension is introduced in this scenario by using the same drop duration D for all users and averaging the exposure maps over 6 min. In this work we set the value of D to 1 s, thus requiring 360 iterations to get an average exposure map.

7.5.1. *Users*

A pool of user equipments (UEs), i.e. terminals, is created in the urban environnement. UEs are randomly distributed on the ground and inside buildings with a ratio (for the same footprint) of 80% indoor UEs and 20% outdoor UEs. There are far more UEs in this pool than real users, in order to represent moving UEs and changing receiving conditions. In each environment described in this study, 640 UEs were generated (540 indoor, 100 outdoor), see Figure 5.

7.5.2. *Beamforming*

In this study we use zero-forcing beamforming [12]. It aims at maximizing the SINR (signal to interference and noise ratio) to serve a maximum number of UEs simultaneously. The beamforming weights applied to each sub-element are obtained by computing the pseudo-inverse of the channel matrix between the 64 sub-elements of the antenna and a set of N UEs ($N \leq 64$). The channel matrix is computed with the simulation method; each channel is the result of multiple paths contributions.

A greedy user selection algorithm is used to find the number K of UEs that can be served simultaneously amongst the N UEs with the overall higher rate with a given noise. Power allocation between users is done with a water-filling method. It is worth noting that K is not an actuel parameter here, as it is automatically computed (usually 3 or 4). An example of beamforming for 3 users simultaneously is illustrated on Figure 5.

7.5.3. *Full algorithm*

- UEs are handled by batches of 64 UEs. First these 64 UEs are removed from the pool of UEs (keeping the ratio between indoor and outdoor UEs, hence 50 indoor UEs and 14 outdoor UEs). Beamforming is performed on the 64 UEs by successive iterations, until every UE has been served (each UE has the same drop duration D). Hence

for each iteration i of beamforming, K_i UEs are served, with their allocated power. An exposure map is computed for each iteration, corresponding to the full antenna power.
- Once the 64 UEs have served, 64 others are extracted from the pool and so one, until the pool empties.
- When the pool is empty, an average (over the total number of iterations and also over time since D is constant) exposure map is computed.

The downlink rate for each UEs is computed but is not used yet, as a constant drop duration is considered for each UE. Each iteration, serving K_i UEs has a 1 s duration.

8. Results and analysis

8.1. *About results*

There are three urban environments and four scenarios in this work. Each scenario allows us to compute an exposure map of the antenna for all receiver points (1.5 m above the ground and on building facades). This exposure map is either directly computed from average diagrams (scenarios 0 and 0′), averaged from multiple simulations of several beams (scenarios 1 and 1′), or averaged over 6 min (scenario 2).

The cumulated distribution function (cdf) of the electric field is then computed for each scenario, for both ground and facade exposure.

8.2. *Preliminary results*

First we compare scenarios 0 (map with average diagram) and 1 (average of maps for each diagram). As expected the mean error between them is very close to zero. Nevertheless the error on some isolated points can be quite high. For instance the interference (either constructive or destructive) between direct and reflected field is amplified in scenario 0 due to the conservative diagram (with a far larger main lobe). Results for five highly exposed points (expressed in V/m) are shown on Table 1.

One important conclusion is that with an average diagram it is not necessary to perform an advanced simulation (with reflections for instance) since it introduces more error and decreases the accurray (scenario 0 without reflection gives results closer to scenario 1).

8.3. *Comparisons between scenarios*

For each urban environment, we compare the cumulated distribution function of electric field levels (in V/m) of the four antenna modelling scenarios. Cumulative distribution functions are calculated by averaging results on receivers for ground maps anf for building facade maps. This allows us to determine both the maximum value and the shape of the distribution function.

8.3.1. *On the ground (outdoor exposure)*

See Figure 6.

8.3.2. *On the facades (indoor exposure)*

See Figure 7.

8.3.3. *Analysis*

In all the cases of this study, the differences between scenario 0 (*a priori* average diagram of all beams) and scenario 1 (*a posteriori* average of all maps, with one map per beam) are significant,

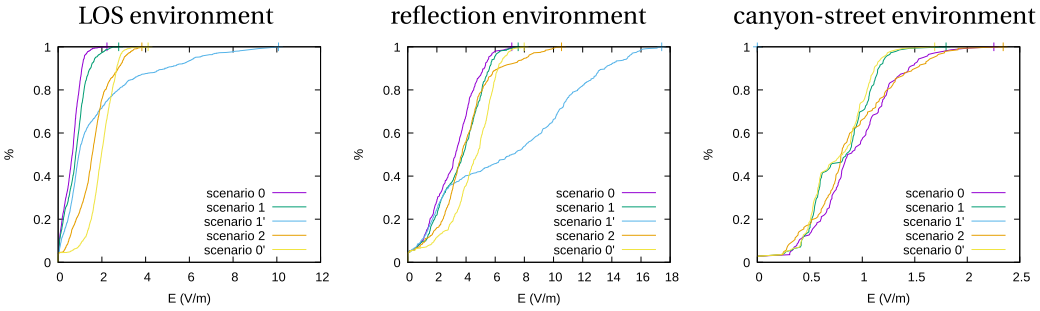

Figure 6. Comparisons between scenarios 0, 0′, 1, 1′ and 2, on the ground for the three environments.

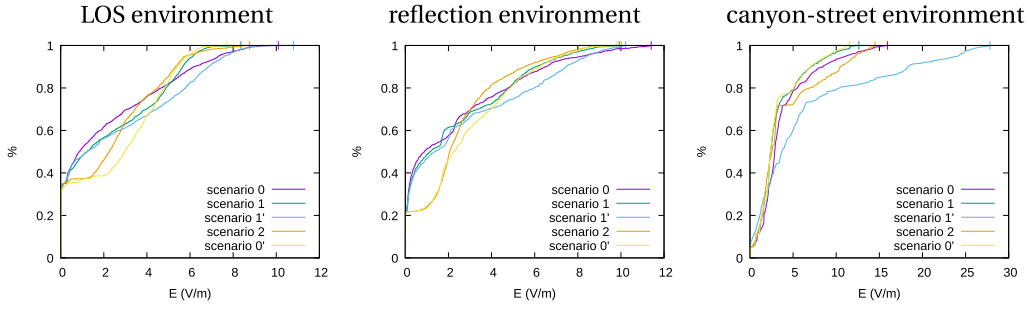

Figure 7. Comparisons between scenarios 0, 0′, 1, 1′ and 2, on the facades for the three environments.

Table 1. Differences between scenarios 0 and 1 at a few selected points with high exposure levels, with ($r = 2$) and without ($r = 0$) reflections taken into account

	#464		#100		#224		#202		#325	
Point	$r = 2$	$r = 0$	$r = 2$	$r = 0$	$r = 2$	$r = 0$	$r = 2$	$r = 0$	$r = 2$	$r = 0$
Scenario 0	4.41	7.44	4.51	7.29	4.56	6.99	6.44	7.37	6.45	6.72
Scenario 1	8.24	7.39	8.04	7.22	7.23	6.92	7.58	7.29	7.44	7.68

first concerning the shape of the distribution function of the electric field, and second concerning the maximum exposure level. In some cases the difference can reach 20%. The use of an average diagram has an influence on the characterization of the exposure levels, specially when there is a significant range of beam directions and changing beam shapes (with the appearance of non-negligible side lobes). This result should be confirmed with manufacturer antenna diagrams for which attenuation values of the side lobes would be available.

Most of the time, scenario 1′ (average of the maps for the beams in line of sight of the exposition areas) is a maximizing one. But it can be matched (for its maximum level) by scenario 2 in open range areas. In fact, the latter can form beams independently of direct visibility, in shadow areas or via reflected multi-paths.

The comparison between scenarios 0′ (ANFR guidelines) and 2 (dynamic beamforming) is what mainly interests us in this study. In all our case studies, scenario 2 gives maximum exposure levels higher or similar to scenario 0′. The usage assumptions of this study surely have a large influence on scenario 2: constant distribution of users at ground level and in buildings (this

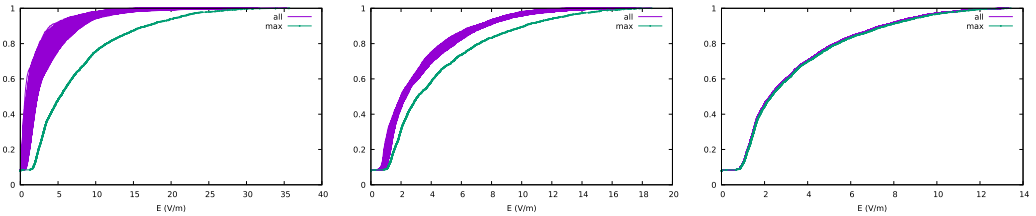

Figure 8. cdf of electric field, averaged over 6 min, for different drop durations D : D = 1 min (left), D = 10 s (middle) and D = 1 s (right).

could depend on the time of day), equal service (in assigned time) among all users, continuous service (antenna at full load). However, the differences between scenarios highlight that the configuration of the antenna environment has an influence on the exposure levels, which does not appear in the use of a scenario with a medium diagram, such as scenario 0 or 0′.

8.3.4. *Influence of drop duration*

On Figure 8 we illustrate the effect of the drop duration D on the cdf of the electric field. A sliding average over 6 min is used to get exposure maps as functions of time. We compare the cdf of all exposure maps (in magenta) with the cdf of the maximum exposure level at any point (in cyan). With D = 1 s, 6 min are enough to get a stable exposure level while for larger D values a longer averaging duration would be needed.

9. Conclusion and future work

By comparing the scenarios based on the use of an average diagram (scenarios 0 and 0′) with a scenario based on the average of the maps for all beams (scenario 1), it appeared that, in the case of beamforming antennas, taking into account the side lobes is essential to obtain a relevant characterization of the exposure levels. This is particularly the case for an antenna having a wide horizontal angular steering range. This conclusion should be refined and confirmed with more complete information from the manufacturers on the diagrams of the 5G antennas that will be field-deployed.

To make the calculation of exposure levels more precise and take into account the antenna environment, it is possible to implement in existing exposure tools a simple scenario which limits the focusing of the beams towards the points of exposure in line of sight of the antenna (scenario 1′). This scenario logically leads to a strong overestimation of the exposure in the majority of the cases studied. This result justifies the use and analysis of a more advanced scenario such as the scenario integrating dynamic beamforming, including the characteristics of the channel between the antenna and the users (scenario 2).

The study of the statistical distribution of the electric field levels shows that the scenarios based on an average diagram, including the scenario adopted for the ANFR guidelines, tend to overestimate the low electric field levels and under estimate the high levels, compared with the scenario incorporating dynamic beamforming (scenario 2). Here again, the statistical distribution of the electric field level shows the advantage of numerical modeling which considers both the environment of the antenna and its realistic behavior in channel estimation. The corollary of this conclusion is that accurately modeling the specific environment of the antenna (buildings, obstacles, etc.) for the numerical modeling of the exposure is of little interest with a simple hypothesis of a generic average antenna diagram.

This first study on a few sites therefore highlights the limitations of an overly simplified statistical approach for modeling the exposure due to smart antennas. These conclusions could

be confirmed by the study of larger sites, with more antennas and base stations and in larger-scale urban environments. The study could also be improved with access to more complete manufacturer data, on antennas actually deployed by telecom operators in the coming months. Future work could also focus on the spatial distribution of electric field, to go beyond the analysis of cumulated distribution functions of electric field levels. Preliminary works already show that this spatial distribution is strongly influenced by the environment.

Finally this study should be carried out on a larger scale. This would make it possible to analyze the shadowed areas (exposure "behind" the buildings in line of sight), areas located at a greater distance from the antenna, and more complex environments with several antennas and base stations. It is important to note that the level of exposure on the facade is the level outside but that the channel was formed with users located inside buildings (taking into account attenuation by the building walls). It should be noted that the methodology implemented in this study can be deployed operationally on any site, and requires calculation resources similar to those of a conventional calculation of exposure levels (only the diagrams of antennas are changed dynamically).

Acknowledgement

This work was partly funded by ANFR.

References

[1] S. Wang, J. Wiart, "Sensor-aided EMF exposure assessments in an urban environment using artificial neural networks", *Int. J. Environ. Res. Public Health* **17** (2020), article no. 3052.

[2] C. Regrain, J. Caudeville, R. de Seze, M. Guedda, A. Chobineh, P. Doncker, L. Petrillo, E. Chiaramello, M. Parazzini, W. Joseph, S. Aerts, A. Huss, J. Wiart, "Design of an integrated platform for mapping residential exposure to Rf-Emf sources", *Int. J. Environ. Res. Public Health* **17** (2020), article no. 5339.

[3] P. Combeau, N. Noé, S. Joumessi, F. Gaudaire, J.-B. Dufour, "A numerical simulation system for mobile telephony base station EMF exposure using smartphones as probes and a genetic algorithm to improve accuracy", *Prog. Electromagn. Res. B* **87** (2020), p. 111-129.

[4] S. Aerts, J. Wiart, L. Martens, W. Joseph, "Assessment of long-term spatio-temporal radiofrequency electromagnetic field exposure", *Environ. Res.* **161** (2017), p. 136-143.

[5] E. Degirmenci, B. Thors, C. Törnevik, "Assessment of compliance with RF EMF exposure limits: approximate methods for radio base station products utilizing array antennas with beam-forming capabilities", *IEEE Trans. Electromag. Compat.* **58** (2016), no. 4, p. 1110-1117.

[6] B. Thors, D. Colombi, Z. Ying, T. Bolin, C. Törnevik, "Exposure to RF EMF from array antennas in 5G mobile communication equipment", *IEEE Access* **4** (2016), p. 7469-7478.

[7] B. Thors, A. Furuskär, D. Colombi, C. Törnevik, "Time-averaged realistic maximum power levels for the assessment of radio frequency exposure for 5G radio base stations using massive MIMO", *IEEE Access* **5** (2017), p. 19711-19719.

[8] P. Baracca, A. Weber, T. Wild, C. Grangeat, "A statistical approach for RF exposure compliance boundary assessment in massive MIMO systems", in *WSA 2018; 22nd International ITG Workshop on Smart Antennas (Bochum, Germany, March 2018)*, 2018, p. 1-6.

[9] E. C. Commitee, "ECC Report 281: Analysis of the suitability of the regulatory technical conditions for 5G MFCN operation in the 3400–3800 MHz band", Tech. report, CEPT, 2018.

[10] N. Noé, F. Gaudaire, M. Diarra Bousso Lo, "Estimating and reducing uncertainties in ray-tracing techniques for electromagnetic field exposure in urban areas", in *2013 IEEE-APS Topical Conference on Antennas and Propagation in Wireless Communications (APWC) (Turin, Italy)*, IEEE, 2013, p. 652-655.

[11] ANFR, "Lignes directrices nationales sur la présentation des résultats de simulation de l'exposition aux ondes émises par les installations radioélectriques", Tech. report, ANFR, October 2019, https://www.anfr.fr/fileadmin/mediatheque/documents/expace/20191001-Lignes-directrices-nationales.pdf.

[12] N. S. G. Dimic, "On downlink beamforming with greedy user selection: performance analysis and a simple new algorithm", *IEEE Trans. Signal Process.* **53** (2015), no. 10, p. 3857-3868.